Centrifugal Distortion Analysis and Pressure Broadening Studies for *l*-Type Doublet Transitions of Cyanoacetylene-^{15}N in the Microwave Range

J. Haekel and H. Mäder

Abteilung Chemische Physik im Institut für Physikalische Chemie der Universität Kiel

Z. Naturforsch. **43a**, 1111–1118 (1988); received September 17, 1988

With the help of Fourier transform spectrometers in the range from 8 GHz to 26.5 GHz, *l*-type doublet transitions of HCCC^{15}N in the first excited state of the degenerate bending vibration v_7, with $36 \leq J \leq 65$, have been investigated. The *J*-dependence of the resonance frequencies was analysed to yield the doubling constant $q^{(0)}$ together with the correction terms $q^{(1)}$ and $q^{(2)}$ due to first and second order contributions from centrifugal distortion. For the lines in X- and Ku-band (8 GHz to 18 GHz) the self-broadening linewidth parameters Γ_p were determined from the pressure dependence of coherence decay rates $1/T_2$ of the observed transient emission signals, following pulsed microwave excitation. For the lines with $J = 36$ and 41, foreign gas broadening in mixtures of HCCC^{15}N with H_2, D_2 and He has also been studied. The experimental results are compared with theoretical predictions, based on a perturbative treatment of binary collisions.

I. Introduction

Studies of *l*-type doublet transitions in the microwave range for linear and symmetric-top molecules have been carried out so far mainly to determine the doubling constant for degenerate vibrational modes with a vibrational angular momentum $l \cdot \hbar$ along the symmetry axis, in some cases with inclusion of centrifugal distortion terms. These investigations provide information about the *intramolecular* Coriolis interaction between vibration and rotation, which removes the $\pm l$-degeneracy of the rovibrational energy levels.

Information about *intermolecular* interaction may be obtained from the study of collision-induced effects such as the pressure broadening of lines. Only few linewidth studies of direct *l*-type doublet transitions have been carried out in the microwave region, like for OCS [1] and HCN [2–4], employing both frequency and time domain techniques. In comparison to the more common investigations of the self-broadening of pure rotational lines, these studies provide additional information about rotational relaxation because the collision-induced energy transfer is different for the following reasons.

Firstly, the collision partners for (absorber) molecules in the investigated *l*-doublet states are mainly (perturber) molecules in the vibrational ground state, i.e. the states of the colliding absorber-perturber pairs are predominantly different. Secondly, first order dipole-type collisional selection rules require a parity change of the involved states [5], which for example excludes $\Delta J = 0$ collisional transitions for linear molecules in the vibrational ground state. For *l*-doublet states, *J*-preserving collisions are allowed in the first order dipole approximation. Finally, pure rotational transitions $J \rightarrow J+1$ in the microwave range cover only a range of few *J*-values, which are normally small with respect to the rotational quantum number *J* for *l*-type doublet transitions in the microwave region. Higher rotational states and thus perturber molecules in states J_2 close to *J* are usually more populated at room temperature for the latter transitions. As consequence, contributions from collision-induced transitions like $J \rightarrow J \pm 1$, $J_2 = J \pm 1 \rightarrow J$ for the absorber-pertuber pair, i.e. collisions with near resonant exchange of rotational energy and thereby significant cross sections, are more weighted for *l*-type doublet transitions.

In this paper, we report the results from microwave studies on *l*-type doublet transitions of HCCC^{15}N in the first excited degenerate bending vibrational state $v_7 = 1^1$, covering the frequency range from 8 GHz to 26.5 GHz. The experimental technique is shortly described in the next section. The results from the centrifugal distortion analysis of the *l*-doublet transition frequencies are given in Section III. The pressure

Reprint requests to Prof. Dr. H. Mäder, Abteilung Chemische Physik im Institut für Physikalische Chemie der Universität Kiel, Olshausenstr. 40–60, D-2300 Kiel, FRG.

0932-0784 / 88 / 1200-1111 $ 01.30/0. – Please order a reprint rather than making your own copy.

broadening studies are reported and discussed in Section IV. The conclusion of the paper is summarized in the last section. Possible line shape distortions due to the 1-bit A/D conversion in data acquisition of the noisy signals are discussed in the Appendix.

II. Experimental

The transient emission technique has been used to determine center frequencies and halfwidths of *l*-type doublet lines of HCCC^{15}N with rotational quantum number J in the range from 36 to 65, employing microwave Fourier transform spectrometers in X- [6], Ku- [7] and K-band [8]. This time-domain technique involves the detection of the transient emission signal which follows the polarization of the gas sample by a short intense microwave pulse. The molecular emission signal oscillates with the resonance frequency of the excited transition and decays at a rate $1/T_2$ which is related to the pressure broadened halfwidth Γ $(=1/2\pi T_2)$ of the line. The signal was frequency-down converted to about 30 MHz intermediate beat frequency by superheterodyne detection and sampled by means of a 1-bit A/D conversion at a rate of 100 MHz, i.e. 10 ns sample intervals. The use of a 1-bit A/D converter in data acquisition requires signal-to-noise ratios well below unity in order to obtain undistorted signals as discussed in the appendix. A total of 1024 data points were sampled, and the results from consecutive experiments were accumulated in the 16-bit memory of a digital averager to achieve signal-to-noise improvement.

A sample of HCCC^{15}N with 95% isotopic enrichment was used after vacuum distillation in the experiments. The ^{15}N- instead of the normal isotopomer of HCCCN was chosen for our study to avoid complications from hyperfine splittings due to the ^{14}N-nuclear quadrupole coupling. The 5% abundance of the normal isotopomer is thought to have no significant influence on the results on the pressure dependence of the halfwidth for the studied lines. All pressure measurements were made with a capacitance manometer (MKS Baratron 310B). For the linewidth studies, the pressure was varied from about 1 mTorr to 7 mTorr (1 mTorr = 0.1333 Pa) for the pure gas. The partial pressures for the foreign gases (H_2, D_2 and He) as used for the investigation of the mixtures, were varied in the range from 1 mTorr to 70 mTorr. All measurements were done at an ambient temperature of $T = 300 \pm 2$ K.

The averaged transient emission signal was analysed by a least squares fitting procedure according to the expression

$$S(t) = S_0 \exp(-t^2/4q^2) \exp(-t/T_2) \cos(2\pi \nu_i t + \Phi), \quad (1)$$

with S_0, T_2, ν_i and Φ as fitting parameters. In (1), $S(t)$ is the value of the signal at the time t after the end of the microwave pulse, $1/T_2$ is the decay rate due to collisions, ν_i corresponds to the transition frequency, and q is related to the Doppler halfwidth $\Delta\nu_D$ $[=\sqrt{\ln 2}/2\pi q]$ of the line. According to our experimental setup, the frequency offset of the observed beat frequency with respect to the 30 MHz intermediate frequency equals the frequency difference between the resonance frequency ν_0 of the transition and the frequency of the polarizing microwave radiation. With the fit results for ν_i and $1/T_2$, partly determined at different pressures, the data on the line center frequencies (see Sect. III) and the pressure dependence of halfwidths (see Sect. IV) are then readily obtained.

III. Centrifugal Distortion Analysis

As far as the pressure broadening of the *l*-type doublet lines was studied (see Sect. IV), the transition frequencies were derived from the fit of the beat frequency in (1). Since no significant pressure-induced lineshift was observed, the average value from measurements at different pressures for each line was taken for the further analysis. All other lines were recorded only at a fixed pressure, and the line center frequencies were then determined with analysis of the power spectrum obtained by Fourier transformation of the transient emission signal to the frequency domain. The resulting values coincide within an accuracy of better than 5 kHz with the fit results from time domain signal analysis. This agreement is not surprising since significant distortions of power spectra, which are mainly due to overlapping lines [9, 10], are absent in the present study.

All observed frequencies are summarized in Table 1, with one more digit given for the averaged fit results obtained by variation of the sample pressure. The *l*-type doublet transition with $J = 53$ is not given since the corresponding emission signal was strongly perturbed by the presence of the nearby $J = 1 \rightarrow 2$ rotational transition in the vibrational ground state.

The experimental resonance frequencies for *l*-type doublet transitions may be approximated by the ex-

Table 1. *l*-Type doublet transition frequencies for HCCC^{15}N in the vibrational state $v_7 = 1^1$. *J*: rotational quantum number; ν_0(obs.): observed frequency; ν_0(calc.) calculated frequencies with use of (2) and constants in Table 2.

J	ν_0(obs.) [MHz]	ν_0(calc.) [MHz]	ν_0(obs.)−ν_0(calc.) [kHz]
36	8242.2073	8242.2075	−0.2
37	8698.5534	8698.5560	−2.6
38	9167.0685	9167.0691	−0.6
39	9647.7343	9647.7334	0.9
40	10140.5343	10140.5351	−0.8
41	10645.4617	10645.4603	1.4
42	11162.4960	11162.4944	1.6
43	11691.6232	11691.6229	0.3
44	12232.8270	12232.8306	−3.6
45	12786.1056	12786.1022	3.4
46	13351.4210	13351.4220	−1.0
47	13928.7766	13928.7739	2.7
48	14518.1434	14518.1417	1.7
49	15119.5060	15119.5086	−2.6
50	15732.8584	15732.8577	0.7
51	16358.1718	16358.1717	0.1
52	16995.4332	16995.4330	0.2
53	[a]	17644.6236	–
54	18305.724	18305.7254	−1.4
55	18978.719	18978.7198	−0.8
56	19663.588	19663.5880	0.0
57	20360.311	20360.3108	0.2
58	21068.867	21068.8687	−1.7
59	21789.243	21789.2421	0.9
60	22521.411	22521.4108	0.2
61	23265.355	23265.3545	0.5
62	24021.052	24021.0527	−0.7
63	24788.485	24788.4853	0.7
64	25567.629	25567.6281	0.9
65	26358.462	26358.4627	−0.7

[a] not measured

pression [11]

$$\nu_0 = q^{(0)}\, J(J+1) - q^{(1)}\, J^2(J+1)^2 + q^{(2)}\, J^3(J+1)^3 - + \ldots, \qquad (2)$$

where $q^{(0)}$ is the *l*-type doubling constant for the considered vibrational mode and $q^{(1)}, q^{(2)}, \ldots$ are correction terms from effects of centrifugal distortion. A least squares fit analysis of the observed frequencies was carried out using (2) with inclusion of $q^{(0)}$, $q^{(1)}$ and $q^{(2)}$. The close agreement between experimental and theoretical values (see Table 1) is clearly shown with the resulting 1.6 kHz root mean square deviation of the fit. The residuals in Table 1 are purely statistical, and no improvement of the fit was obtained with inclusion of higher order terms in (2).

The fit results for the *l*-type doubling constants are given in Table 2 and compared with available previous data for both HCCC^{15}N [12] and HCCC^{14}N [13, 14]. The observed slight decrease of the values for the ^{15}N-isotopomer with respect to the normal species may be explained qualitatively with the decrease of the vibrational frequency upon ^{15}N-substitution, which reduces the effects of Coriolis interaction. As far as the doubling constant $q^{(0)}$ is concerned, it is roughly inverse proportional to the vibrational frequency [11]. From the results in Table 2 one may then estimate the fundamental frequency of the v_7 vibrational mode of HCCC^{15}N to be shifted to about 220 cm^{-1}, i.e. about two wavenumbers below the corresponding frequency for HCCC^{14}N at 222.4 cm^{-1} [15].

Table 2. *l*-Type doublet constants for the vibrational mode v_7 of HCCC^{15}N. The errors in parantheses are in the last digit given and equal twice the standard deviation for this work.

Molecule	Ref.	$q^{(0)}$ [MHz]	$q^{(1)}$ [MHz] $\cdot 10^{-6}$	$q^{(2)}$ [MHz] $\cdot 10^{-12}$
HCCC^{15}N	this work	6.207801 (28)	15.0572 (10)	51.72 (17)
HCCC^{15}N	[12]	6.205 (26)	–	–
HCCC^{14}N	[13]	6.538254 (33)	15.983 (12)	–
HCCC^{14}N	[14]	6.53864 (2)	16.32 (2)	67 (5)

IV. Pressure Broadening Studies

For a part of the studied *l*-type doublet lines the pressure broadening parameters were derived from a least squares fit analysis of transient emission signals according to (1), yielding the relaxation rate $1/T_2$ at different sample pressures. The coefficients for the linear pressure dependence of $1/T_2$ were then obtained by a linear regression analysis, weighting the $1/T_2$ data points according to their standard deviations in the expression

$$1/T_2 = \alpha + \beta\, p \quad . \qquad (3)$$

For the pure gas, p is the total sample pressure and α mainly accounts for wall collisions. For the binary mixtures, p is the foreign gas partial pressure and α contains a contribution from self-collisions of cyanoacetylene at a fixed amount. The resulting rate coefficients β are finally converted to the more familiar pressure broadening parameter Γ_p ($=\beta/2\pi$).

Pressure broadening of most of the *l*-type doublet lines in X- and Ku-band has been studied for the pure gas. The analysis of transient emission signals was carried out for all lines with $36 \leq J \leq 52$ except for the

Table 3. Halfwidth parameter Γ_p due to self- and foreign gas broadening of l-type doublet lines of HCCC^{15}N in the vibrational state $v_7 = 1^1$ at room temperature (300 ± 2 K). J: rotational quantum number; Γ_p (obs.): observed halfwidth parameter; Γ_p (calc.): calculated halfwidth parameter according to modified Murphy-Boggs theory. The errors in parantheses are in the last digit given and equal twice the standard deviation.

Perturber	J	Γ_p (obs.) [MHz/Torr]	Γ_p (calc.) [MHz/Torr]
HCCC^{15}N	36	63.2 (18)	86.6
	37	64.4 (10)	85.3
	38	62.5 (10)	83.9
	39	60.5 (8)	82.4
	40	62.4 (7)	80.9
	41	58.4 (11)	79.2
	42	[a]	77.5
	43	60.3 (23)	75.8
	44	[a]	74.0
	45	47.9 (16)	72.1
	46	[a]	70.3
	47	50.2 (10)	68.3
	48	45.8 (4)	66.4
	49	[a]	64.5
	50	44.7 (8)	62.6
	51	43.0 (7)	60.7
	52	42.0 (9)	58.7
H_2	36	8.24 (6)	6.11
	41	8.18 (16)	6.09
D_2	36	6.65 (10)	5.03
	41	6.62 (16)	4.99
He	36	4.04 (6)	2.85
	41	4.03 (6)	2.84

[a] not measured.

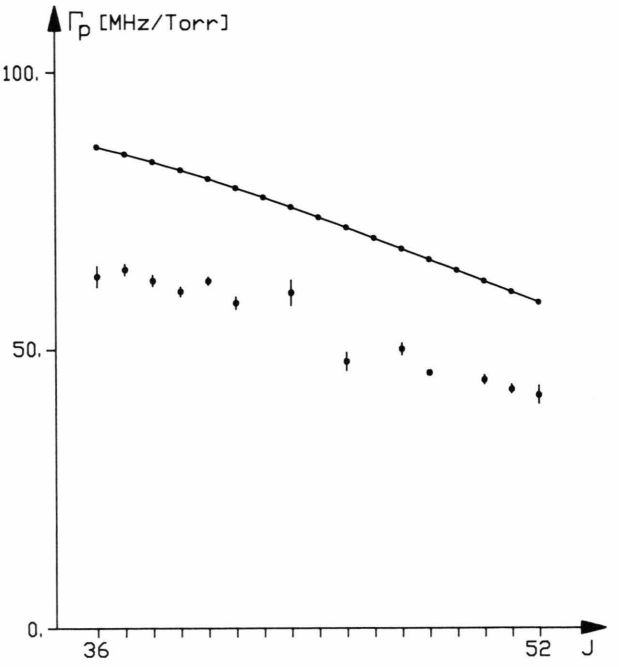

Fig. 1. Self-broadening linewidth parameters Γ_p [MHz/Torr] for l-type doublet transitions of HCCC^{15}N in the vibrational state $v_7 = 1^1$ versus rotational quantum number J associated with the l-doublet states. Points with error bars give experimental values with twice the standard deviation. Points connected by solid line give theoretical results (for details see text).

transitions with $J = 42$, 44, 46, and 49, which were perturbed by emission signals from other lines. For the mixtures of HCCC^{15}N with H_2, D_2 and He, the l-type doublet lines with $J = 36$ and $J = 41$, respectively, were investigated.

The experimental results for the pressure broadening coefficient Γ_p due to self- and foreign gas collisions are given in Table 3. The quoted errors are twice the standard deviations from the linear least squares fit and do not reflect systematic deviations from pressure inaccuracies, shifts in temperature (< 2 K) and additional partial pressure inaccuracies for the mixtures.

Table 3 gives also the results from theoretical predictions for Γ_p, using the modified Murphy-Boggs theory [16] which employs a perturbative approach to treat the binary collision dynamics. The calculations were based on a long-range intermolecular interaction potential, considering attractive forces due to permanent multipole moments (dipole moment for HCCC^{15}N and quadrupole moment for HCCC^{15}N, H_2 and D_2), induction and dispersion interaction. The molecular constants which were used for characterization of the interaction potential are summarized in Table 4. Since rather high J-states of HCCC^{15}N are involved, a first order centrifugal distortion correction was included in the calculation of the rotational energy levels.

Considering the results for the pure gas in Table 3, the pressure broadening parameter Γ_p clearly decreases with increasing rotational quantum number J both for the experimental and theoretical values, as illustrated also in Figure 1. However, the calculations predict linewidths about 35%–40% greater than experimentally observed.

The observed J-dependence of the self-broadening parameter Γ_p mainly reflects the Boltzmann distribution of the population of perturber rotational energy levels in the vibrational ground state. The fraction f_{J_2} of perturber molecules with rotational quantum number J_2 before a collision weights the corresponding

Table 4. Molecular parameters for the interaction potential used in the theoretical calculations. B: rotational constant; D: first order centrifugal distortion constant, μ: electric dipole moment; Q: electric quadrupole moment; IP: ionization potential; $\alpha_{av}=(\alpha_{\parallel}+2\alpha_{\perp})/3$: average polarizability; $\alpha_{an}=(\alpha_{\parallel}-\alpha_{\perp})$: polarizability anisotropy.

Absorber or perturber	Vibrational state	B [GHz]	D [kHz]	μ [D]	Q [D·Å]	IP [eV]	α_{av} [Å^3]	α_{an} [Å^3]
HCCC^{15}N	ground	4.416753[a]	0.510[a]	3.733[d]	4.624[e]	11.0[f]	5.28[g]	6.04[g]
HCCC^{15}N	$v_7=1^1$	4.430758[b]	0.532[c]	3.727[d]	4.624[e]	11.0[f]	5.28[g]	6.04[g]
H_2	ground	1823.01[h]	–	–	0.663[i]	15.43[j]	0.79[g]	0.22[g]
D_2	ground	912.24[h]	–	–	0.663[k]	15.46[j]	0.79[k]	0.22[k]
He	–	–	–	–	–	24.46[j]	0.20[l]	–

[a] [13]. – [b] Evaluated from the *l*-type doublet components of the $J=1$–2 rotational transition.
[c] Estimated from vibrational state dependence of D for the ^{14}N-isotopomer [13]. – [d] [17].
[e] According to different definitions for Q, twice the value as given in [18] for the ground vibronic state.
[f] Estimated from values for similar compounds [19]. – [g] [20]. – [h] [21]. – [i] [22]. – [j] [19]. – [k] Value for H_2. – [l] [4].

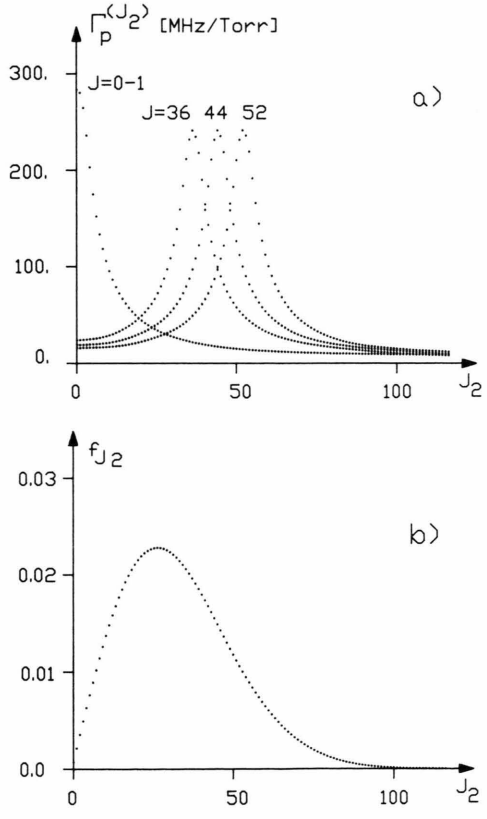

Fig. 2. a) Plot of $\Gamma_p^{(J_2)}$ [MHz/Torr] for the HCCC^{15}N–HCCC^{15}N system versus the perturber rotational quantum number J_2 for the *l*-type doublet transitions of HCCC^{15}N in the vibrational state $v_7=1^1$ with $J=36$, 44, 52 and the rotational transition $J=0$–1 in the vibrational ground state: b) Fraction of perturber molecules f_{J_2} in the vibrational ground state of HCCC^{15}N versus the rotational quantum number J_2.

contribution $\Gamma_p^{(J_2)}$ to the total linewidth according to

$$\Gamma_p=\sum_{J_2} f_{J_2}\,\Gamma_p^{(J_2)}. \tag{4}$$

As an example, theoretical results for the J_2-dependence of $\Gamma_p^{(J_2)}$ are shown in Fig. 2 for the *l*-type doublet transitions of HCCC^{15}N with $J=36$, 44 and 52, together with the Boltzmann distribution f_{J_2}. For comparison, a plot of $\Gamma_p^{(J_2)}$ for the $J=0$–1 pure rotational transition in the vibrational ground state is also given.

With consideration of Fig. 2, it may be noted that for each *l*-type doublet transition with rotational quantum number J, the curves $\Gamma_p^{(J_2)}$ are peaked around $J_2=J$. This indicates the predominant contributions from collisions with near resonant exchange of rotational energy to the broadening of the lines. The most significant contributions are then expected to be caused by collision-induced transitions $J\rightarrow J\pm1$, $J_2=J\pm1\rightarrow J$ for the absorber-perturber pair, according to first order dipole-type collisional selection rules [5].

Collisions of the type $J\rightarrow J\pm1$, $J_2=J\rightarrow J\mp1$ are similarly important since the mismatch between pre- and postcollisional sum of rotational energies of the collision partners ($\approx 2B$) is still sufficiently small to make the concept of rotationally resonant collisions approximately applicable. For larger rotational constants and thus a larger energy mismatch, the corresponding collision-induced transition probability may be reduced significantly to yield a dip in the $\Gamma_p^{(J_2)}$ curves at $J_2=J$. Unlike calculated here for HCCCN, this behaviour was indeed predicted in case of *l*-type

transitions of HCN [4], for which the rotational constant is about ten times larger.

A similar resonance effect is found for pure rotational transitions, as seen for example from the plot of $\Gamma_p^{(J_2)}$ for the $J=0-1$ transition in the vibrational ground state. However, since the fraction f_{J_2} of perturber molecules with low values of J_2 is comparatively small, the resulting linewidth parameter (theoretical value: 39.0 MHz/Torr; experimental value [23]: 33.0 (20) MHz/Torr) is considerably smaller than for the l-type doublet transitions studied here. The J-dependence of the latter transitions is primarily due to the weight function f_{J_2} in (4), since apart from a shift of the center peaks at $J=J_2$, the curves $\Gamma_p^{(J_2)}$ are not much different. As the maximum of the Boltzmann distribution curve is at about $J=26$ at room temperature, one would expect the linewidth parameters for l-type doublet transitions to be at maximum at around $J=26$. We were not able to test this experimentally because the transition frequency for the corresponding l-type doublet transition (≈ 4.35 GHz) is out of the range of our spectrometers.

Discrepancies between experimental and theoretical values for linewidth parameters due to self-broadening have also been found for l-type doublet transition of OCS [1] and HCN [4], respectively, with theoretical values about 40% and 15% larger than the experimental results. A better agreement was obtained in case of HCN by a proper scaling of the theoretical values, using a normalization scheme of transition probabilities [4]. Such a procedure is, however, arbitrarily included in the theory and has therefore not been used here.

As far as the long-range attractive part of the intermolecular potential is concerned, dipole-dipole interaction predominantly contributes to the cross-sections for T_2-relaxation because of the large dipole moment of HCCCN. This has been tested by omitting higher order interaction terms in the numerical calculations, which reduced the theoretical linewidth parameters by less than 1%. Accordingly, most of the HCCCN–HCCCN collisions may be considered to be weak collisions for which the conversion from rotational to translational energy is small and the classical straight-line trajectory approximation is expected to be good [5]. It has been argued that, within the weak collision limit, a nonperturbative approach to collision theory would reduce the resulting linewidth parameter in particular with contribution from perturber molecules in higher J-states [24]. It is therefore believed that the systematic discrepancies between theory and experiment are more likely due to the perturbative approach used here, rather than to an inaccurate potential surface.

Considering the results for the mixtures in Table 3, no significant J-dependence is found for both the experimental and theoretical values. However the agreement between theory and experiment is rather poor, as indicated by predicted linewidths about 25% to 30% smaller than experimentally observed. This discrepancy may be because of the breakdown of the assumptions made in the theory, like the weak collision approximation, and/or an inaccurate intermolecular potential function.

We finally mention that calculations which took also HCCC^{15}N perturbers in the vibrational state $v_7=1^1$ into account, did not significantly change the results. Further, the $\Delta J=0$ collision-induced transitions within the l-type doublet states were found to contribute less than 1.4% to the self-broadening of lines. The corresponding transitions in case of foreign gas broadening are more important, contributing up to 22% to the calculated width parameter.

V. Conclusion

We have reported results from centrifugal distortion analysis and pressure broadening studies for l-type doublet transitions of HCCC^{15}N in the vibrational state $v_7=1^1$ for different rotational quantum numbers J. Up to second order, centrifugal distortion terms have been determined accurately and close agreement between experimental and theoretical resonance frequencies has been obtained. Linewidth parameters have been obtained from the pressure dependence of transient emission decay rates for the pure gas and in mixtures with H_2. D_2 and He. The observed J-dependence of the pure gas results could be explained qualitatively with consideration of the Boltzmann population distribution of perturber rotational states. However, the discrepancy between experimental and theoretical results for the studied systems indicates the insufficiency of the used modified Murphy-Boggs theory to treat the binary collisions.

Acknowledgements

We thank all members of the group, especially Prof. H. Dreizler, for help and discussion. We would also

like to express our appreciation to Dr. S. C. Mehrotra for many advices concerning the theoretical treatment of pressure broadening. The financial support from the Deutsche Forschungsgemeinschaft and the Fonds der Chemischen Industrie is gratefully acknowledged.

Appendix

Analyzing the averaged transient decay signal, it is normally assumed that the original molecular signal is faithfully traced. However, due to one-bit averaging of the noisy signals, the resulting lineshape is distorted in case of too strong signals. The following treatment summarizes earlier discussions of these effects [25, 26], emphasizing particularly the resulting accuracy limitations of relaxation rates $1/T_2$.

Let the time-dependent input voltage of the 1-bit comparator be represented by a superposition of the molecular signal $U_S(t)$ and a noise voltage with a Gaussian distribution of the amplitudes and a characteristic $(1/e)$-width U_N. Then, the normalized distribution function of the input voltage is given by [25, 26]

$$W(U) = (1/U_N\sqrt{\pi}) \exp\{-(U-U_S)^2/U_N^2\}. \quad \text{(A.1)}$$

The probabilities p_+ and p_- to encounter a positive or negative input voltage, respectively, is the given by

$$p_\pm = \tfrac{1}{2} \pm \tfrac{1}{2} \operatorname{erf}(U_S/U_N), \quad \text{(A.2)}$$

where erf denotes the error-function.

A total of 1024 data points are sampled in our experiments, and either $+1$ or -1 is added to the corresponding memory cells of the 16-bit averager, depending on the sign of the input voltage. Considering a specific memory address of the averager, corresponding to a fixed time delay after the end of the microwave pulse, its final content after M averaging cycles is given by

$$C = M_+ - M_- \quad \text{(A.3)}$$

where M_+ and M_- are the total number of plus- and minus-ones, respectively ($M = M_+ + M_-$). For sufficiently large numbers of repetition cycles M, the distribution of C-values may be approximated again by a Gaussian distribution law [26] which peaks at

$$\bar{C} = M \cdot (p_+ - p_-) = M \cdot \operatorname{erf}(U_S/U_N) \quad \text{(A.4)}$$

and is characterized by a $(1/e)$-width

$$\Delta C = \sqrt{8 M p_+ p_-}\,. \quad \text{(A.5)}$$

In the following we ignore the implications from possible memory overflow [26] and use the most probable value $\bar{C}$ (A.4) of the accumulated signal for the further discussion. Then, if $U_{Si} = U_S(t_i)$ denotes the signal as time t_i after the end of the microwave pulse, the corresponding averaged signal C_i is according to (A.4) given by

$$\bar{C}_i = M \cdot \operatorname{erf}(U_{Si}/U_N) \quad \text{(A.6)}$$

which is used in data analysis to evaluate the relaxation rate $1/T_2$ according to (1). However, since (1) describes only the time dependence of U_S, the resulting rates may be incorrect, as the values $\bar{C}_i$ are not strictly proportional to the original signal amplitudes. Only if $U_{Si} \ll U_N$ holds for all values of i, the error-function in (A.6) may be approximated by $(2/\sqrt{\pi})(U_{Si}/U_N)$. As consequence, reliable values for $1/T_2$ are obtained from the analysis of the averaged data. For stronger signals, which may occur in particular shortly after the end of the polarizing pulse, this approximation is no longer valid and the resulting $\bar{C}_i$-values are smaller than predicted from (1) ($\operatorname{erf}(U_{Si}/U_N) < (2/\sqrt{\pi})(U_{Si}/U_N)$). This behaviour then leads to $1/T_2$ rates from analysis of averaged data which are apparently too small.

For our purpose to discuss the accuracy of the results for $1/T_2$ it is sufficient to consider here a simplified expression for the time dependence of transient emission signals, namely

$$U_S(t) = A \cdot \exp(-t/T_2) \quad \text{(A.7)}$$

which ignores signal oscillations and minor contributions from Doppler dephasing, thus describing only the envelope of the oscillating decay function (1) or a transient emission signal at zero beat frequency.

According to (A.7) the relaxation rate $1/T_2$ may be derived from the signal amplitudes U_{S1} and U_{S2} at two different times t_1 and t_2, respectively,

$$1/T_2 = \ln(U_{S1}/U_{S2})/(t_1 - t_2). \quad \text{(A.8)}$$

The corresponding averaged signal values $\bar{C}_1$ and $\bar{C}_2$, respectively, give the apparent rate $1/\tilde{T}_2$,

$$1/\tilde{T}_2 = \ln(\bar{C}_1/\bar{C}_2)/(t_1 - t_2)\,. \quad \text{(A.9)}$$

In order to get an estimate for the deviation of $1/\tilde{T}_2$ from $1/T_2$ we define the ratio

$$k = (1/\tilde{T}_2) : (1/T_2) = \ln(\bar{C}_1/\bar{C}_2) : \ln(U_{S1}/U_{S2})\,. \quad \text{(A.10)}$$

If both U_{S1} and U_{S2} are very small with respect to U_N we have $\bar{C}_1/\bar{C}_2 \approx U_{S1}/U_{S2}$ (see previous discussion) and thus $k \approx 1$. For stronger signals a lower limit of k

Table A1. Comparison of apparent ($1/\tilde{T}_2$) and true ($1/T_2$) relaxation rates in case of one-bit averaging of noisy decay signals for different signal-to-noise ratios U_S/U_N. $k = (1/\tilde{T}_2) : (1/T_2)$ lower limit for the ratio of both rates; dev = $100 \cdot (1-k)$ upper limit for the relative percentage error of the apparent relaxation rate.

U_S/U_N	0.02	0.04	0.06	0.08	0.10	0.15	0.20	0.25	0.30	0.40	0.50	0.75	1.00
k	0.9999	0.9990	0.9976	0.9957	0.9934	0.9851	0.9736	0.9590	0.9414	0.8978	0.8442	0.6780	0.4926
dev [%]	0.0	0.1	0.2	0.4	0.7	1.5	2.6	4.1	5.1	10.2	15.6	32.2	50.7

may be obtained with use of the approximation $t_2 - t_1 \ll T_2$, which implies that $U_{S1} - U_{S2} = \delta U_S \ll U_{S1}$ and $\bar{C}_1 - \bar{C}_2 = \delta\bar{C} \ll \bar{C}_1$. Then, we may rewrite k, setting $U_{S2} = U_S$ and $\bar{C}_2 = \bar{C}$ in (A.10):

$$k = \ln(1 + \delta\bar{C}/\bar{C}) : \ln(1 + \delta U_S/U_S) \approx (\delta\bar{C}/\bar{C}) : (\delta U_S/U_S). \tag{A.11}$$

Using the definition (A.6) of $\bar{C}$, k is approximately given by

$$\begin{aligned} k &\approx (\delta\bar{C}/\delta U_S) : (\bar{C}/U_S) \\ &\approx (2/\sqrt{\pi})\,(U_S/U_N)\exp\{-(U_S/U_N)^2\}/\mathrm{erf}(U_S/U_N) \end{aligned} \tag{A.12}$$

Some combinations of values for k and U_S/U_N have been calculated according to (A.12) and are listed in Table A1 together with the corresponding relative error of the resulting $1/T_2$ rates. As seen from the Table, k approaches unity for $U_S \ll U_N$, but for larger signals the error of $1/T_2$ becomes large. It should be noted, however, that the corresponding k-values give only a lower limit to estimate the accuracy of the results. When carrying out the actual data analysis more than two values are taken into consideration, from which a part may arise from molecular signals which are buried more in noise. As consequence, more favourable k-values or smaller errors of the rates will result from the analysis of the averaged signals. However, since the stronger signals are more weighted in the least squares fit analysis of the experimental data, one has to make sure of a sufficiently low signal-to-noise ratio in order to obtain reliable data on spectral parameters.

[1] S. C. Mehrotra and H. Mäder, Can. J. Phys. **62,** 1280 (1984).
[2] J. B. Cohen and E. B. Wilson, J. Chem. Phys. **58,** 442 (1973).
[3] M. Charron, T. G. Anderson, and J. I. Steinfeld, J. Chem. Phys. **73,** 1494 (1980).
[4] S. C. Mehrotra, H. Mäder, J.P.M. de Vreede, and H. A. Dijkerman, Chem. Phys. **93**, 115 (1985).
[5] T. Oka, Adv. At. Mol. Phys. **9,** 127 (1973).
[6] G. Bestmann and H. Dreizler, Z. Naturforsch. **37a,** 58 (1982).
[7] G. Bestmann, H. Dreizler, H. Mäder, and U. Andresen, Z. Naturforsch. **35a,** 392 (1980).
[8] W. Stahl, G. Bestmann, H. Dreizler, U. Andresen, and R. Schwarz, Rev. Sci. Instrum. **56,** 1759 (1985).
[9] I. Merke and H. Dreizler, Z. Naturforsch. **43a,** 196 (1988).
[10] J. Haekel and H. Mäder, Z. Naturforsch. **43a,** 203 (1988).
[11] W. Gordy and R. L. Cook, in: Microwave Molecular Spectra, J. Wiley & Sons, Chapter V, New York 1984.
[12] P. D. Mallinson and R. L. de Zafra, Mol. Phys. **36,** 827 (1978).
[13] W. J. Lafferty and F. J. Lovas, J. Phys. Chem. Ref. Data **7,** 441 (1978).
[14] R. L. de Leon and J. S. Muenter, J. Chem. Phys. **82,** 1702 (1985).
[15] P. D. Mallinson and A. Fayt, Mol. Phys. **32,** 473 (1976).
[16] S. C. Mehrotra and J. E. Boggs, J. Chem. Phys. **66**, 5306 (1977).
[17] P. Wolf and H. Mäder, J. Mol. Struct., in press (1988).
[18] W. H. Stolze and D. H. Sutter, Z. Naturforsch. **39a,** 1092 (1984).
[19] Handbook of Chemistry and Physics, 65th ed. CRC Press Inc., p. E-70ff, Boca Raton 1985.
[20] J. O. Hirschfelder, C. F. Curtiss, and R. B. Bird, Molecular Theory of Gases and Liquids, p. 948ff, J. Wiley & Sons, New York 1950.
[21] G. Herzberg, Spectra of Diatomic Molecules 2nd ed., p. 501ff, D. van Norstrand, Princeton 1963.
[22] D. E. Stogryn and A. P. Stogryn, Mol. Phys. **11,** 371 (1966).
[23] S.C.Mehrotra, H. Dreizler and H. Mäder, J. Quant. Spectrosc. Radiat. Transfer **34,** 229 (1985).
[24] S.C.Mehrotra and J. E. Boggs, J. Chem. Phys. **63,** 1453 (1975).
[25] J. Haekel, Diplom thesis, Kiel 1985.
[26] B. Kleinbömer and D. H. Sutter, Z. Naturforsch. **43a,** 561 (1988).